

Supporting Information

Non-Halogen-Solvent-Processed Highly Efficient Organic Solar Cells with a Record Open Circuit Voltage Enabled by Noncovalent-Locked Novel Polymer Donors

Hui Guo^a, Youdi Zhang^{a,d}, Lie Chen^{*a}, Xunfan Liao^c, Qian Xie^a, Yongjie Cui^c, Bin Huang^{a,d}, Changduk Yang^{*d}, and Yiwang Chen^{*a,b}

^a College of Chemistry/Institute of Polymers and Energy Chemistry (IPEC),
Nanchang University, Nanchang 330031, (P. R. China).

^b Institute of Advanced Scientific Research (iASR), Jiangxi Normal University, 99
Ziyang Avenue, Nanchang 330022, China.

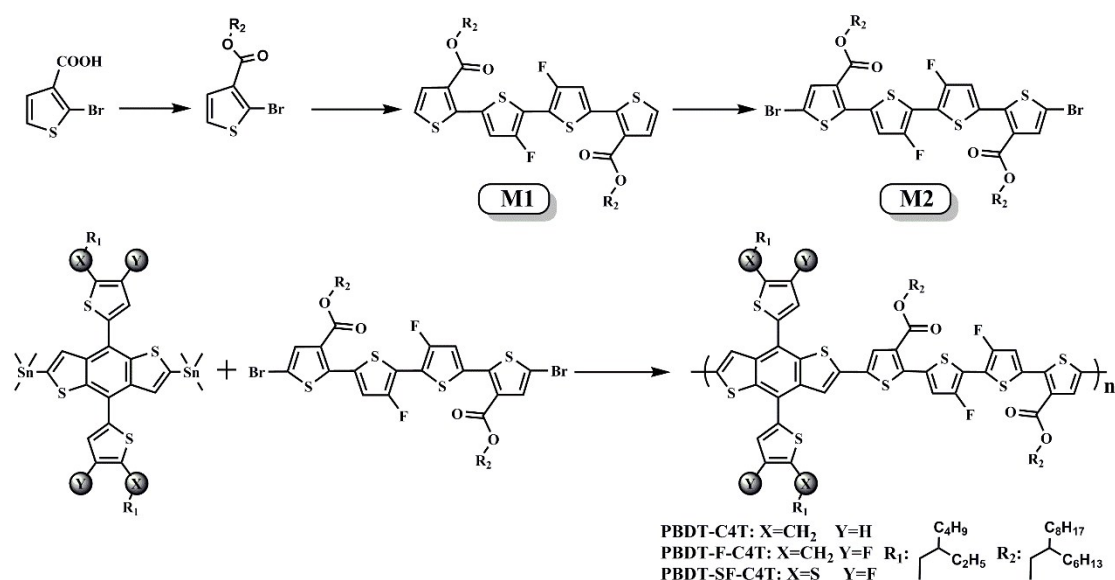
^c State Key Laboratory for Modification of Chemical Fibers and Polymer Materials
(SKLFPM), College of Materials Science and Engineering, Donghua University, 2999
Renmin Bei Road, Shanghai 201620, China

^d Department of Energy Engineering, School of Energy and Chemical Engineering,
Perovtronics Research Center, Low Dimensional Carbon Materials Center, Ulsan
National Institute of Science and Technology (UNIST), 50 UNIST-gil, Ulju-gun,
Ulsan 44919, South Korea.

1. Materials and Synthetic of Methods

Materials: All reagents and solvents, unless otherwise specified, were purchased from Alfa, (3,3'-difluoro-[2,2'-bithiophene]-5,5'-diyl)bis(trimethylstannane) was purchased from derthon optoelectronic materials science technology, Aldrich and Solarmer Materials Inc. and were used without further purification. IT-4F and benzodithiophene (BDT) were purchased from SunaTech Inc.. Indium-tin oxide (ITO) glass was purchased from Delta Technologies Limited, Tetrakis(triphenylphosphine)palladium(0) Pd(PPh₃)₄ was obtained from J&K.

Synthetic of Methods



Scheme S1. The synthetic route of the polymers.

Synthesis of 2-hexyldecyl 2-bromothiophene-3-carboxylate:

2-bromo-3-thiophenecarboxylic acid (1.32 g, 6.37 mmol), 1-bromo-2-hexyldecyl (5.84 g, 19.01 mmol), potassium carbonate (4 g, 28.94 mmol) and N, N-dimethylformamide (DMF, 15 ml) were added to a 100 ml round bottom flask. The mixture was stirred for 40 h at 80 °C, then cool down to room temperature, 30 mL water was added, extracted with dichloromethane (CH₂Cl₂). The organic phase was dried with sodium sulfate; purified with column chromatography on silica gel using hexane/CH₂Cl₂, yielding the pure compound as colorless oil (2.47 g, 90 %). ¹H NMR (400 MHz, cdcl₃) δ 7.36 (d, *J* = 5.8 Hz, 2H), 7.25 (s, 1H), 7.21 (d, *J* = 5.8 Hz, 2H), 4.19 (d, *J* = 5.5 Hz,

5H).

Synthesis of bis(2-hexyldecyl) 3'',4'-difluoro-[2,2':5',2'':5'',2''''-quaterthiophene]-3, 3''''-dicarboxylate (M1):

2-hexyldecyl 2-bromothiophene-3-carboxylate (1 g, 2.32 mmol) and (3, 3'-difluoro-[2, 2'-bithiophene]-5, 5'-diyl) bis (trimethylstannane) (0.48g, 0.9 mmol) in dry toluene (10 mL) was degassed thrice with nitrogen followed by the addition of Pd (PPh₃)₄ (85 mg, 0.065 mmol), After being stirred at 110 °C for 72 h under nitrogen, the reaction mixture was cooled to room temperature and then dissolved in CH₂Cl₂, washed with water and dried by anhydrous magnesium sulfate. After evaporation of the solvent, the crude product was purified by column chromatography on silica gel using hexane/CH₂Cl₂ as eluent and get a yellow oily liquid (0.66 g, 81 %). ¹H NMR (400 MHz, CDCl₃) δ (ppm): 7.50 (d, *J* = 5.4 Hz, 1H), 7.33 (s, 1H), 7.23 (s, 1H), 4.17 (d, *J* = 5.6 Hz, 2H), 1.70 (s, 1H), 1.56 (s, 2H), 1.38 – 1.17 (m, 31H), 0.86 (t, *J* = 6.6 Hz, 8H).

Synthesis of bis(2-hexyldecyl) 5, 5''''-dibromo-3'', 4'-difluoro-[2, 2':5', 2'':5'', 2''''-quaterthiophene]-3, 3''''-dicarboxylate (M2):

M3 (0.5 g, 0.55 mmol) was dissolved in a mixture of chloroform (20 mL) , trifluoroacetic acid (0.5 mL) and NBS (0.3 g, 1.66 mmol) were then added to the solution and stirred for 2 h in the dark. The mixture was extracted with chloroform several times and the organic was combined. The solvent was removed and purified with a flash column chromatography using hexane/CH₂Cl₂ as eluent and get a yellow oily liquid (0.48 g, 83 %). ¹H NMR (400 MHz, CDCl₃) δ (ppm): 7.12 (s, 2H), 6.97 (s, 2H), 4.41-4.68 (d, 4H), 1.87 (s, 2H), 1.16-1.25 (m, 48H), 0.88-0.85 (m, 12H).

Synthesis of PBDT-C4T:

Compound (4,8-bis(5-(2-ethylhexyl)thiophen-2-yl)benzo[1,2-b:4,5-b']dithiophene-2,6-diyl)bis(trimethylstannane) (BDT, 0.180 g, 0.2 mmol) and M2 (0.212 g, 0.2 mmol) were mixed in 10 ml of toluene. After the solution was flushed with N₂ for 5 min, Pd₂(dba)₃ (3.7 mg, 0.004 mmol) and P(o-Tol)₃ (4.9 mg, 0.016 mmol) were added, the mixture was further flushed with N₂ for 10 min. The reactant was heated to reflux for

24 hours. The reactant was cooled to room temperature, and the polymer was precipitated by addition of 100 ml methanol, then filtered through a Soxhlet thimble, extraction with methanol, hexane, and chloroform. The corresponding polymer was obtained as solid powder from the chloroform fraction by precipitation from methanol. After the polymer was dried under vacuum, obtained crimson solid with a yield of ~76 %. ¹H NMR (400 MHz, CDCl₃) δ 7.26 (s, 1H), 4.21 (s, 1H), 3.49 (s, 1H), 2.99 (s, 1H), 2.22 – 0.66 (m, 8H).

Synthesis of PBDT-F-C4T:

Compound (4,8-bis(5-(2-ethylhexyl)-4-fluorothiophen-2-yl)benzo[1,2-b:4,5-b']dithiophene-2,6-diyl)bis(trimethylstannane) (BDT-F, 0.188 g, 0.2 mmol) unit and M2 (0.212 g, 0.2 mmol) were mixed in 10 ml of toluene. After the solution was flushed with N₂ for 5 min, Pd₂(dba)₃ (3.7 mg, 0.004 mmol) and P(o-Tol)₃ (4.9 mg, 0.016 mmol) were added, the mixture was further flushed with N₂ for 10 min. The reactant was heated to reflux for 24 hours. The reactant was cooled to room temperature, and the polymer was precipitated by addition of 100 ml methanol, then filtered through a Soxhlet thimble, extraction with methanol, hexane, and chloroform. The corresponding polymer was obtained as solid powder from the chloroform fraction by precipitation from methanol. After the polymer was dried under vacuum, obtained crimson solid with a yield of ~79 %. ¹H NMR (400 MHz, CDCl₃) δ 7.24 (s, 1H), 3.93 (s, 1H), 3.64 (s, 1H), 3.47 (s, 2H), 3.29 (s, 1H), 1.76 – 0.61 (m, 10H).

Synthesis of PBDT-SF-C4T:

Compound (4,8-bis(4-fluoro-5-(heptan-3-ylthio)thiophen-2-yl)benzo[1,2-b:4,5-b']dithiophene-2,6-diyl)bis(trimethylstannane) (BDT-SF, 0.195 g, 0.2 mmol) unit and M2 (0.212 g, 0.2 mmol) were mixed in 10 ml of toluene. After the solution was flushed with N₂ for 5 min, Pd₂(dba)₃ (3.7 mg, 0.004 mmol) and P(o-Tol)₃ (4.9 mg, 0.016 mmol) were added, the mixture was further flushed with N₂ for 10 min. The reactant was heated to reflux for 24 hours. The reactant was cooled to room temperature, and the polymer was precipitated by addition of 100 ml methanol, then filtered through a Soxhlet thimble, extraction with methanol, hexane, and chloroform. The polymer was obtained from the chloroform fraction by precipitation from methanol. After the

polymer was dried under vacuum, obtained crimson solid with a yield of ~63%. ^1H NMR (400 MHz, CDCl_3) δ 7.26 (s, 1H), 3.49 (s, 1H), 2.99 (s, 1H), 1.06 (d, 13H).

2. Instruments

The ^1H NMR spectra were recorded in deuterated solvents on a Bruker ADVANCE 400 NMR Spectrometer. ^1H NMR chemical shifts were reported in ppm downfield from tetramethylsilane (TMS) reference using the residual protonated solvent as an internal standard. Thermogravimetric analysis (TGA) was carried out on a PerkinElmer TGA instrument for thermal analysis at a heating rate of 10 °C/min under nitrogen. Number-average (M_n) and weight-average (M_w) molecular weights were determined with Waters 2410 gel permeation chromatography (GPC) with a refractive index detector in THF using a calibration of polystyrene standards. UV-vis absorption spectra were recorded on a Perkin Elmer Lambda 750 spectrophotometer. All film samples were spin-cast on ITO substrates. Solution UV-Vis absorption spectra at elevated temperatures also were collected on a Perkin Elmer Lambda 750 Spectrophotometer. Before each measurement, the system was held for at least 10 min at the target temperature to reach thermal equilibrium. A cuvette with a stopper (Sigma Z600628) was used to avoid volatilization during the measurement. Cyclic voltammetry (CV) was performed by a Zahner IM6e electrochemical work station, using Ag/AgCl as the reference electrode, a Pt plate as the counter electrode, and a glassy carbon as the working electrode. Polymers were drop-cast onto the electrode from 1,2,4-trimethylbenzene (TMB) solutions to form thin films. 0.1 mol L⁻¹ tetrabutylammonium hexafluorophosphate in anhydrous acetonitrile was used as the supporting electrolyte. The scan rate was 0.05 V s⁻¹. The specimen for AFM measurements was prepared using the same procedures those for fabricating devices but without MoO₃/Ag on top of the active layer. Transmission electron microscopy (TEM) images were taken on a JEOL-2100F transmission electron microscope and an internal charge-coupled device (CCD) camera. The specimen for TEM measurement was prepared by spin casting the blend solution on ITO/PEDOT: PSS substrate, then floating the film on a water surface, and transferring to TEM grids.

3. Device fabrication

OSCs devices were fabricated with the inverted structure of Glass/ITO/ZnO/active layer/MoO₃/Ag. Specific process is as follows: the etched ITO substrate was ultrasonically cleaned in detergent, water (twice), acetone and isopropanol for 2 hours. After drying, the etched ITO substrate process in UV ozone for 15 minutes and then ZnO was spin-casted onto the ITO. Afterwards, the ITO glass was thermally annealed at 205 °C for 50 minutes. Next, the active layer was spin-casted on the ZnO. Finally, 3 nm MoO₃ and 70 nm Ag layer were deposited by evaporation under a pressure of ca. 4×10^{-4} Pa. The ZnO was spin-coated at 4000 r.p.m. for 1 min. The 1,2,4-trimethylbenzene (TMB) solution and chlorobenzene of polymers: IT-4F stirred at 65 °C overnight (an overall concentration of 20 mg/mL) and spin-coated at 1500 r/min. The chloroform solution of polymers: IT-4F stirred at 40 °C overnight (an overall concentration of 16 mg/mL) and spin-coated at 2000 r/min. Except for the spin coating of the ZnO layer onto the ITO substrate, all photovoltaic device fabrication processes were carried out in nitrogen glove box with oxygen and humidity of less than 4 ppm. The test for this work was still measured in nitrogen glove box. The current–voltage ($J-V$) characteristics were performed by a Keithley 2400 Source Meter (100 mW/cm², AM 1.5 G) and all devices area are 4 mm². The external quantum efficiency (EQE) tests were based on an Oriel Cornerstone monochromator, which was still performed in the nitrogen glove box.

4. SCLC Mobility Measurements

Hole and electron mobility of polymers:IT-4F blend films were measured using the space charge limited current (SCLC) method. Device with a structure of ITO/PEDOT:PSS/Polymers:IT-4F/MoO₃/Ag was used for hole-only measurement and device with a structure of ITO/ZnO/Polymers:IT-4F/PDINO/Al was used for electron-only measurement. The SCLC mobilities were calculated by MOTT-Gurney equation:

$$J = \frac{9}{8} \epsilon_0 \epsilon_r \mu \frac{V^2}{d^3}$$

Note that J is the current density, ϵ_r is the dielectric constant of active layer, ϵ_0 is the vacuum permittivity, μ is the mobility of hole or electron and d is the thickness of the active layer, V is the internal voltage in the device, and $V = V_{\text{appl}} - V_{\text{bi}}$, where V_{appl} is the voltage applied to the device, and V_{bi} is the built-in voltage resulting from the relative work function difference between the two electrodes.

Table S1. OSCs performance metrics for polymer donors:IT-4F photoactive blends.

Donor	LUMO/HOMO	E_g^{opt}	E_{loss}	V_{oc} (V)	J_{sc} (mA cm ⁻²)	FF (%)	PCE (%)	solvent	Ref.
PBTA-TF	-3.42/-5.36 (eV)	1.90	0.76	0.73	20.24	0.72	10.6	CF+DIO	[1]
J91	-3.02/-5.50 (eV)	2.00	0.75	0.78	18.6	55.4	8.04	CB	[2]
L810	-3.58/-5.57 (eV)	1.99	0.74	0.79	20.7	73.5	12.1	CB	[2]
J71	-3.24/-5.40 (eV)	1.96	0.71	0.82	19.38	73.12	11.62	CF	[3]
PCI(4)BDB-T	-3.47/-5.48 (eV)	1.75	0.65	0.84	20.14	71.33	12.11	CB	[4]
PM6	-3.61/-5.50 (eV)	1.82	0.65	0.84	22.2	72.5	13.5	CB/(TA+DIO)	[5]
PBDB-T-2Cl	-3.56/-5.51 (eV)	1.80	0.63	0.86	21.80	0.77	14.4	CB+DIO	[6]
PBDB-TF	-3.65/-5.54 (eV)	1.81	0.66	0.87	20.38	0.77	13.7	CB+DIO	[7]
T1	-3.63/-5.48 (eV)	1.83	0.65	0.88	21.1	0.76	14.2	THF/NMP	[8]
PM7	-3.57/-5.52 (eV)	1.79	0.62	0.88	20.9	71.1	13.1	Tol.	[9]
PDTB-EF-T	-3.59/-5.50(eV)	1.93	0.62	0.90	20.73	0.76	14.2	CB+DIO	[10]
PhI- <i>h</i> BT	-3.80/-5.55 (eV)	1.75	0.61	0.91	19.41	0.76	13.31	CB	[11]
PTO2	-3.67/-5.59 (eV)	2.01	0.59	0.91	21.5	0.75	14.7	CB+DIO	[12]
<i>h</i> PhI- <i>h</i> BT	-3.86/-5.63 (eV)	1.77	0.58	0.94	19.01	0.71	12.74	CB	[11]
PBDT(E)BTz- <i>p</i>	-3.65/-5.65 (eV)	2.02	0.52	0.98	14.38	48.2	6.80	CB	[13]
PBDT(E)BTz- <i>d</i>	-3.68/-5.60 (eV)	2.00	0.55	0.95	14.68	54.5	7.55	CB	[13]
PBDT-F-C4T	-3.55/-5.60 (eV)	1.95	0.55	0.98(0.94)	17.6(19.0)	64.2(70.3)	11.2(12.5)	TMB(TMB+DIO)	This work
PBDT-SF-C4T	-3.60/-5.62 (eV)	1.94	0.54	0.99(0.95)	11.9(16.1)	58.6(65.1)	6.84(9.91)	TMB(TMB+DIO)	This work

a) Average PCEs in brackets for over ten devices.

Thermal Properties of the Polymers

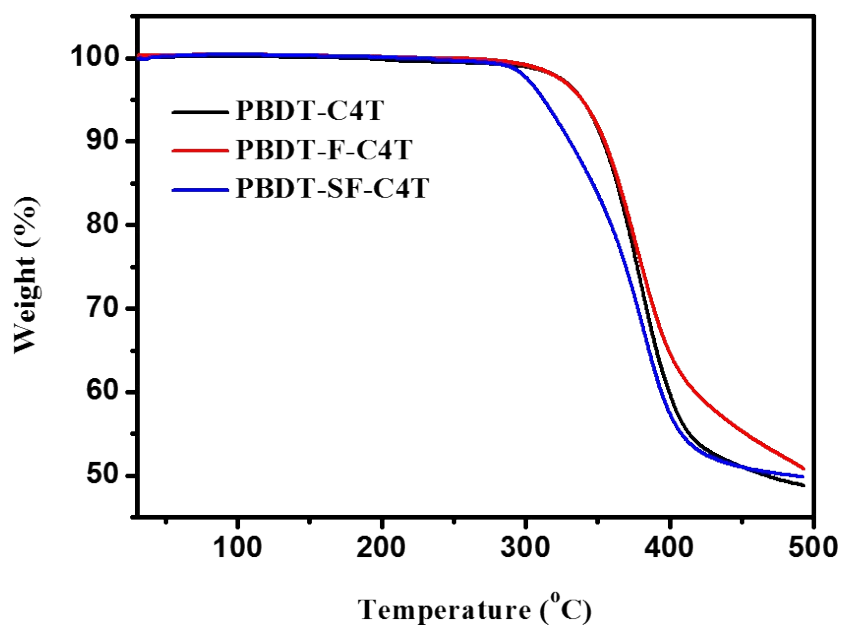


Figure S1. The thermogravimetric analysis (TGA) plot of polymers PBDT-C4T, PBDT-F-C4T and PBDT-SF-C4T with a heating rate of 10 °C min⁻¹ under nitrogen atmosphere.

Absorption of the Polymers

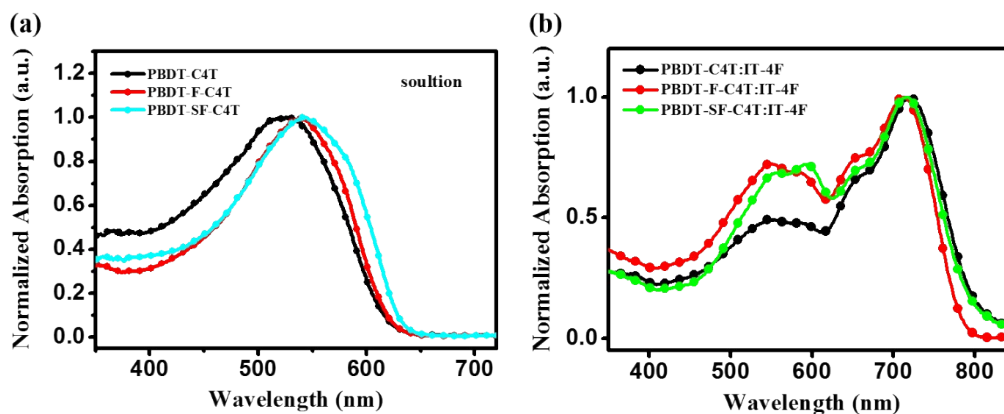


Figure S2. (a) Normalized absorption of solution UV-vis absorption of PBDT-C4T, PBDT-F-C4T and PBDT-SF-C4T; (b) The UV spectra of the polymer donors:IT-4F blend films.

Energy levels calculation

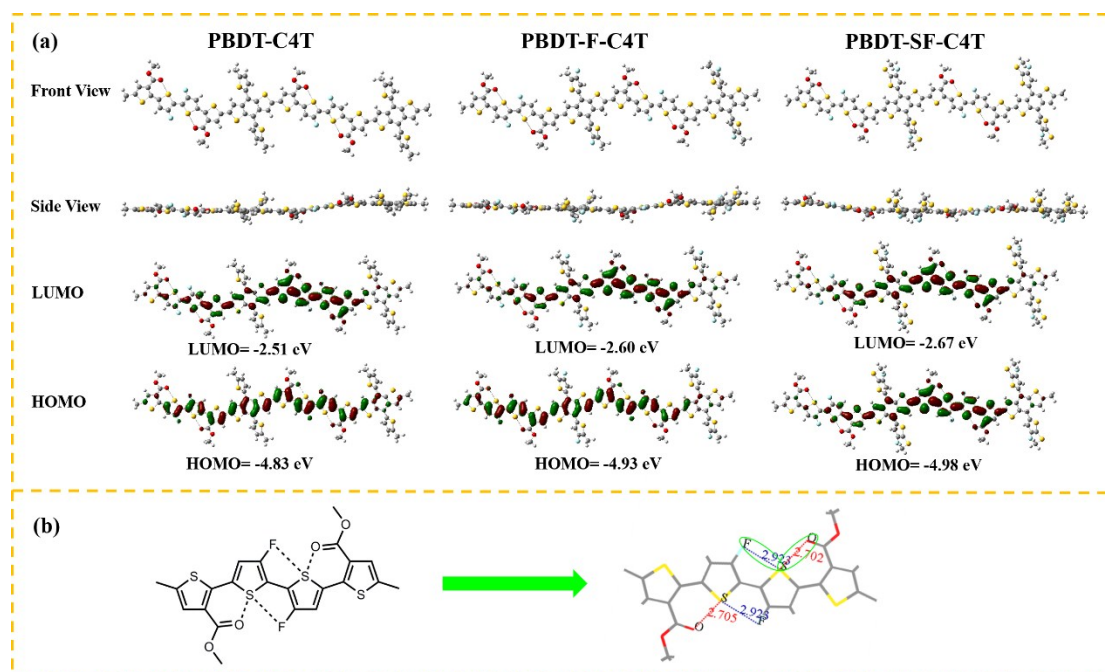


Figure S3. a) The optimized molecular conformation and electron density distributions of the polymers PBDT-C4T, PBDT-F-C4T and PBDT-SF-C4T, performed at the B3LYP/6-31G(d,p); b) the charge analysis of atom-atom distances, performed at the B3LYP/6-31G(d,p).

Cyclic voltammetry Properties of the Polymers

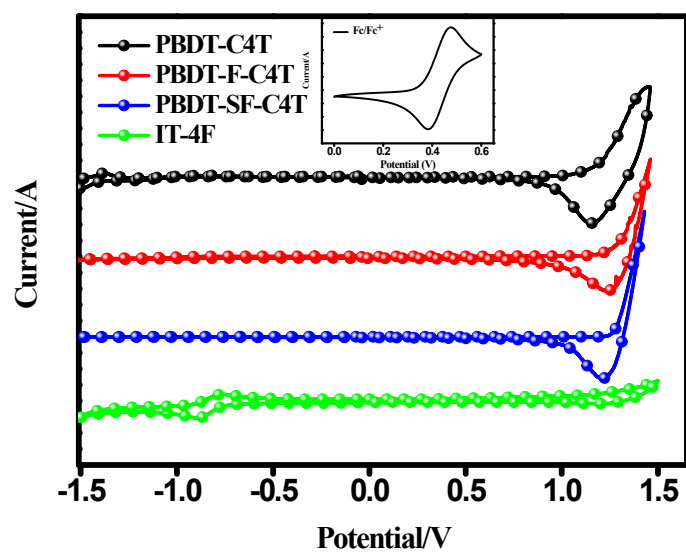


Figure S4. Cyclic voltammetry curve of the polymer PBDT-C4T, PBDT-F-C4T, PBDT-SF-C4T and acceptor IT-4F films in CH₂CH₃CN/0.1 mol/L Bu₄NPF₆ solutions at a scan rate 20 mV/s.

Different Conditions of the Devices Performance

Table S2. Photovoltaic performance parameters of the NF-OSCs based on PBDT-F-C4T: acceptors with different acceptors.

Active layer	V_{oc} (V)	J_{sc} (mA/cm ²)	FF (%)	PCE (%)	Solvent
PBDT-F-C4T:ITIC	1.15	8.91	50.83	5.05	CB
PBDT-F-C4T:ITIC-Th	1.12	10.6	56.64	6.82	CB
PBDT-F-C4T:ITIC-Th1	1.01	10.19	47.92	4.94	CB
PBDT-F-C4T:IT-4F	0.98	15.32	61.81	9.29	CB
PBDT-F-C4T:Y6	0.929	6.15	34.03	1.95	CB

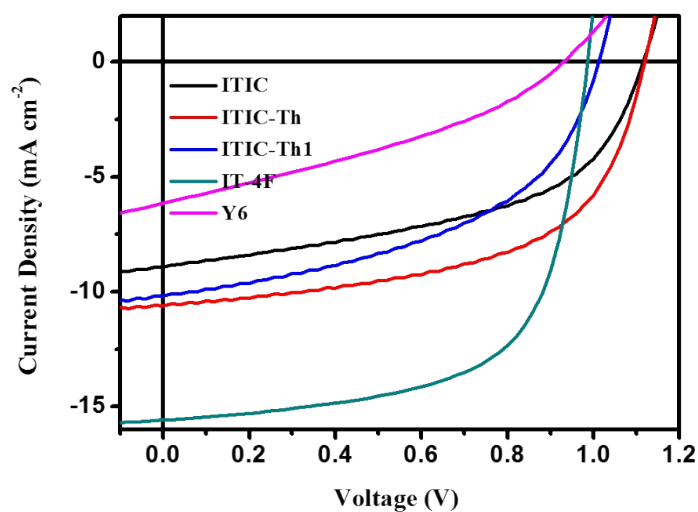


Figure S5. The J - V curves with different acceptors based on PBDT-F-C4T.

Table S3. Photovoltaic performance parameters of the NF-OSCs based on PBDT-F-C4T: IT-4F with different content additive.

Active layer	V_{oc} (V)	J_{sc} (mA cm ⁻²)	FF (%)	PCE (%)	Additive	Solvent
PBDT-F-C4T:IT-4F	0.95	10.19	59.07	5.75	0.5%CN	TMB
PBDT-F-C4T:IT-4F	0.94	9.7	59.1	5.4	1%CN	TMB
PBDT-F-C4T:IT-4F	0.9	13.3	64.1	7.7	1%DIO	TMB
PBDT-F-C4T:IT-4F	0.96	17.12	63.31	10.42	0.25%DIO	TMB

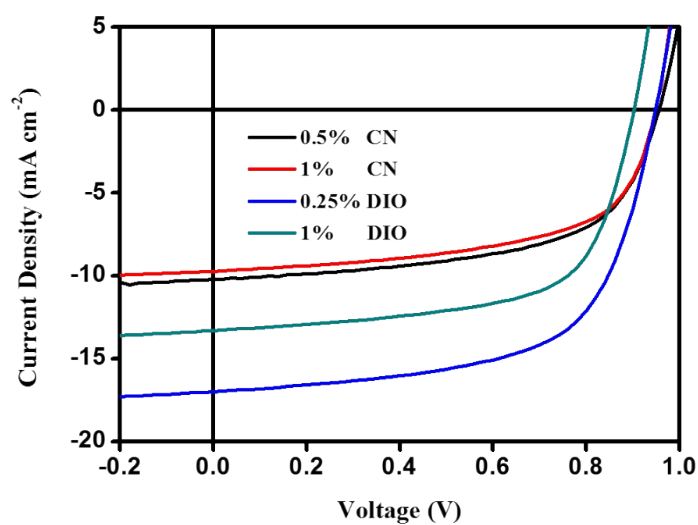


Figure S6. The J - V curves with different content based on PBDT-F-C4T:IT-4F.

Table S4. Photovoltaic performance parameters of the NF-OSCs based on PBDT-F-C4T: IT-4F with different annealing temperature.

Active layer	V_{oc} (V)	J_{sc} (mA cm ⁻²)	FF (%)	PCE (%)	Annealing	Solvent
PBDT-F-C4T:IT-4F	0.95	12.27	59.15	6.9	80	TMB
PBDT-F-C4T:IT-4F	0.95	16.9	60.16	9.7	100	TMB
PBDT-F-C4T:IT-4F	0.95	17.01	64.97	10.53	120	TMB
PBDT-F-C4T:IT-4F	0.94	16.62	66.08	10.37	140	TMB
PBDT-F-C4T:IT-4F	0.88	9.89	51.16	4.45	160	TMB

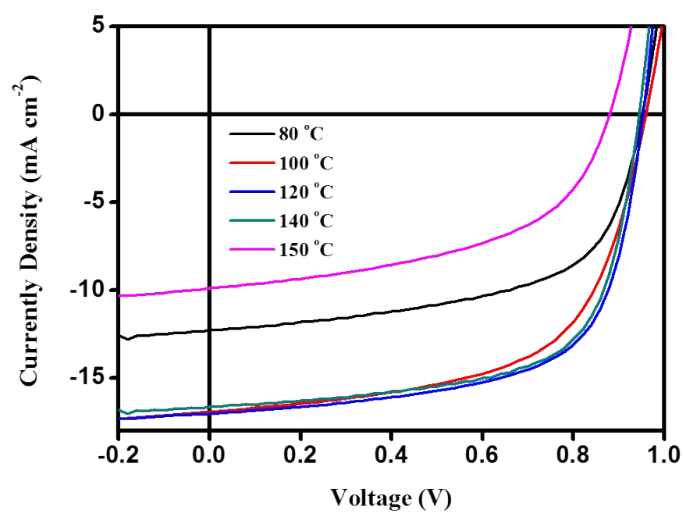


Figure S7. The J - V curves with different annealing temperature (°C) based on PBDT-F-C4T:IT-4F.

Table S5. Photovoltaic performance parameters of the NF-OSCs based on PBDT-F-C4T: IT-4F with different solvent.

Active layer	V_{oc} (V)	J_{sc} (mA cm ⁻²)	FF (%)	PCE (%)	D:A ratios	Solvent
PBDT-F-C4T:IT-4F	0.983	15.32	61.8	9.29	1:1	CB
PBDT-F-C4T:IT-4F	0.988	16.66	66	10.87	1:1	TMB
PBDT-F-C4T:IT-4F	0.991	14.78	51.1	7.22	1:1	CF

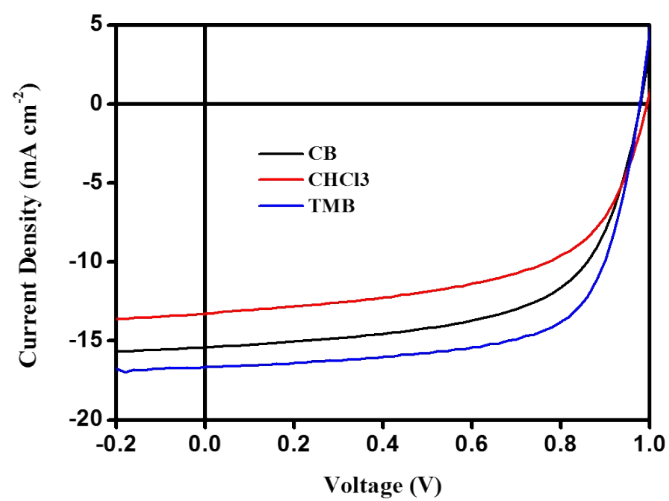


Figure S8 The J - V curves with different solvent based on PBDT-F-C4T:IT-4F.

Table S6. The photovoltaic parameters of different active layer processed by various non-halogenated solvent systems under Air Mass 1.5G, 100 mW cm⁻² illumination.

Donor	Acceptor	<i>V</i> _{oc} (V)	<i>J</i> _{sc} (mA cm ⁻²)	FF (%)	PCE (%)	solvent	Ref.
PBDB-T	IT-M	0.94	17.1	0.72	11.6	XY	[14]
PBQ-4F	ITIC	0.95	17.87	66.8	11.34	THF	[15]
BDTSTNTTR	PC ₇₁ BM	0.93	16.21	76.5	11.5	CS ₂	[16]
PTB7-Th:PTN	PC ₇₁ BM	0.78	21.47	68.31	11.44	ethylbenzene	[17]
PBZ-CISi	IT-4F	0.93	19.2	71.5	12.8	Tol	[18]
PBDTS-TDZ	ITIC	1.10	17.78	65.4	12.80	<i>O</i> -XY	[19]
PBDT-TDZ	ITIC	1.01	17.15	67.7	11.72	<i>O</i> -XY	[19]
PTB-EDOTS	ITIC-Th	0.88	16.25	71.2	10.18	MeTHF	[20]
PBDB-T	IT-M	0.91	12.85	0.53	6.2	THF	[21]
PBDB-T-BO	IT-M	0.97	15.68	0.70	10.64	THF	[21]
PBDB-BzT	IT-M	0.96	17.63	0.69	11.68	THF	[21]
PM6	IT-4F	0.84	20.5	0.75	12.5	XY	[22]
PBTA-TF	IT-M	0.96	18.71	0.70	13.1	XY	[23]
PBTA-TF	IT-M	0.95	18.14	0.66	11.7	THF	[23]
PB3T	IT-M	1.00	18.9	0.63	11.9	anisole	[24]
T1	IT-4F	0.887	21.1	0.76	14.2	THF	[8]
PBDT-F-C4T	IT-4F	0.98(0.94)	17.6(19.0)	64.2(70.3)	11.2(12.5)	TMB(TMB+DIO)	This work
PBDT-SF-C4T	IT-4F	0.99(0.95)	11.9(16.1)	58.6(65.1)	6.84(9.91)	TMB(TMB+DIO)	This work

a) Average PCEs in brackets for over ten devices.

Morphology Properties of the Polymers

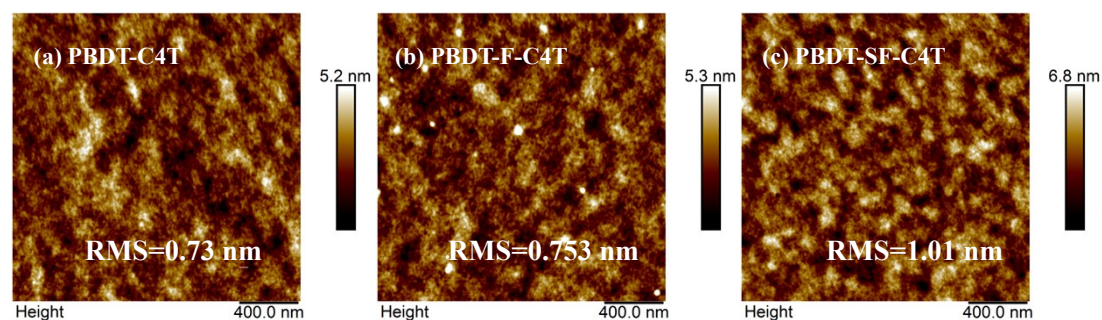


Figure S9. AFM height image of the neat film of PBDT-C4T, PBDT-F-C4T and PBDT-SF-C4T.

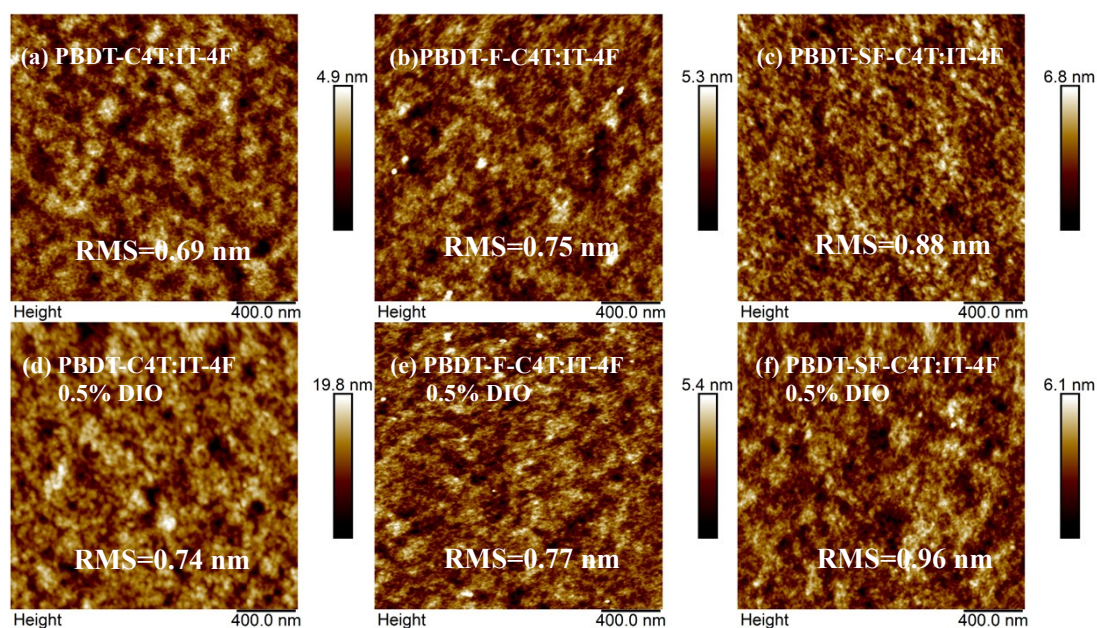


Figure S10. The AFM height images of the a) PBBDT-C4T: IT-4F; b) PBBDT-F-C4T: IT-4F; c) PBBDT-SF-C4T: IT-4F; d) PBBDT-C4T: IT-4F with 0.5% DIO; e) PBBDT-F-C4T: IT-4F with 0.5% DIO; f) PBBDT-SF-C4T: IT-4F with 0.5% DIO blend films.

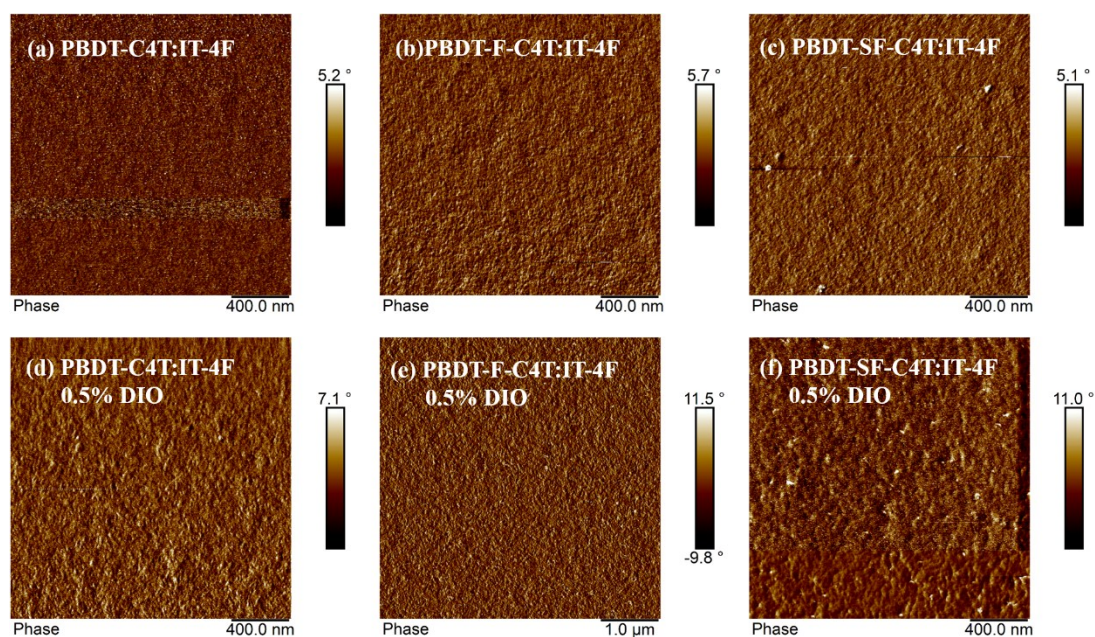


Figure S11. AFM phase image of the copolymer: IT-4F blend films; a) PBBDT-C4T: IT-4F; b) PBBDT-F-C4T:IT-4F; c) PBBDT-SF-C4T:IT-4F; d) PBBDT-C4T:IT-4F with 0.5% DIO; e) PBBDT-F-C4T:IT-4F with 0.5% DIO; f) PBBDT-SF-C4T:IT-4F with 0.5% DIO;

SCLC Mobility Measurements

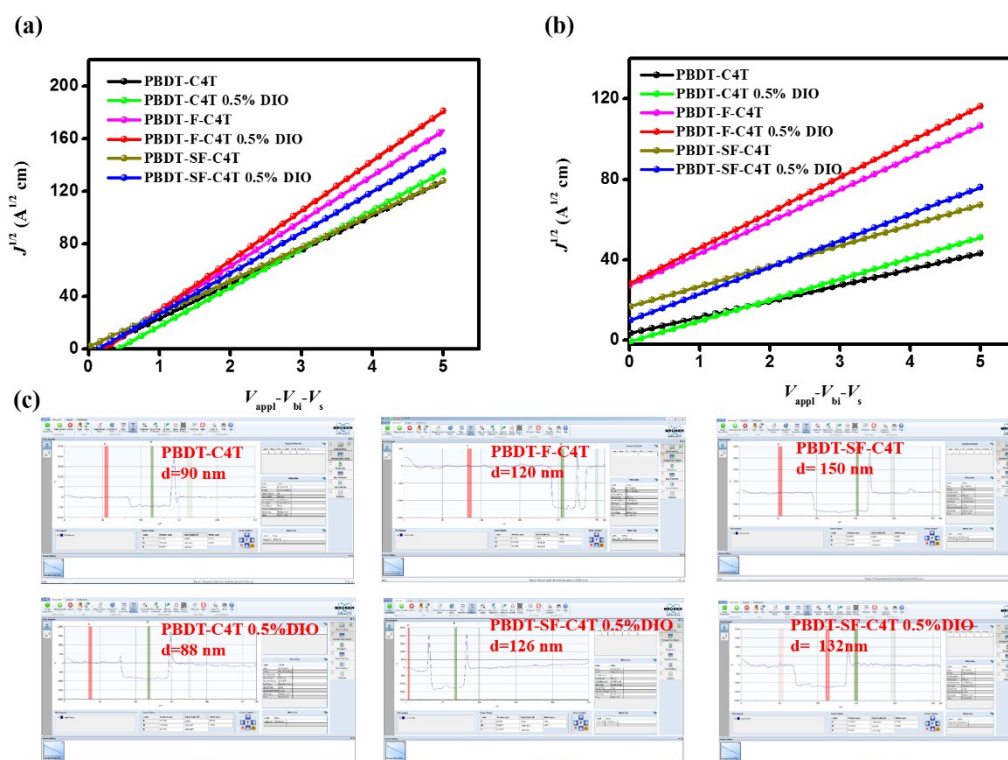


Figure S12. a) The only electron mobilities of the blend films; b) the only hole mobilities of the blend films; c) the film thickness of polymers:IT-4F.

Table S7. Summary of GIWAXS packing parameters.

Entry	q (\AA^{-1})	d-spacing (\AA)	FWHM (\AA^{-1})	Coherence length (\AA)
PBDT-C4T	1.685	3.713	0.232	24.64
PBDT-F-C4T	1.667	3.769	0.226	25.29
PBDT-SF-C4T	1.673	3.756	0.251	22.77
PBDT-C4F:IT-4F	1.752	3.586	0.231	22.48
PBDT-F-C4T:IT-4F	1.758	3.574	0.249	23.57
PBDT-SF-C4T:IT-4F	1.728	3.864	0.237	22.93

^{a)} d-spacing = $2\pi/q$, ^{b)} CCL = $0.9 \times \pi / \text{FWHM}$.

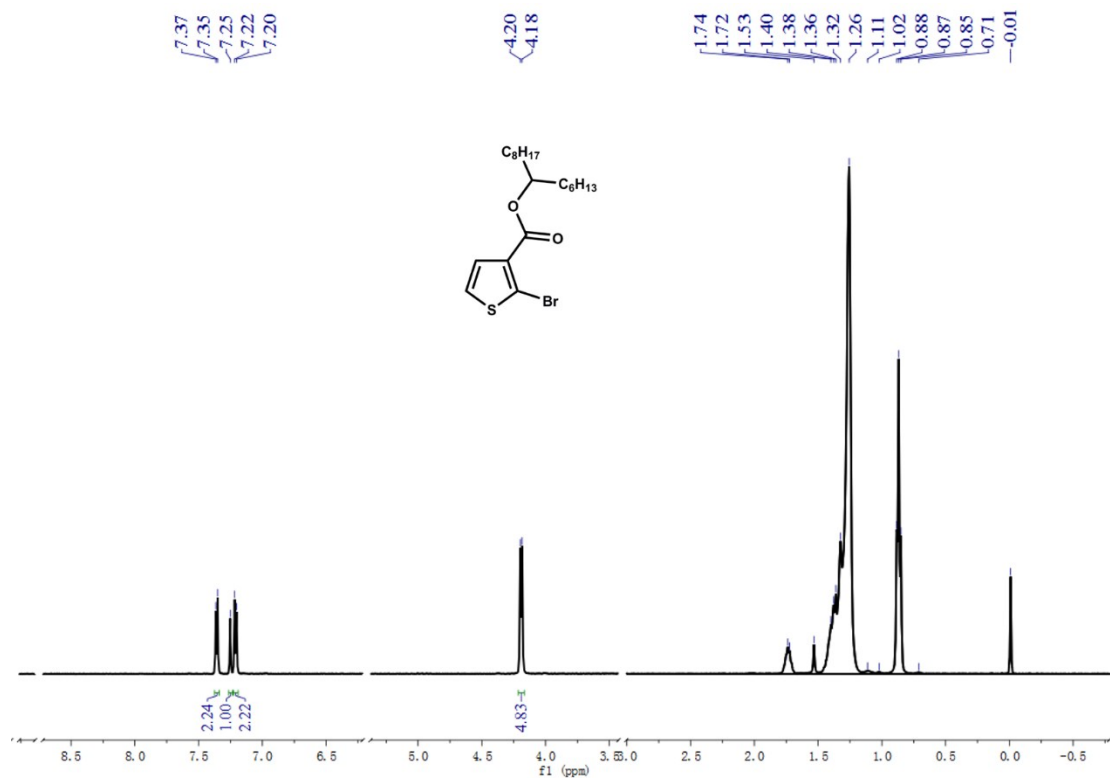


Figure S13. The ¹H NMR of 2-(2-bromothiophen-3-yl)propanoate.

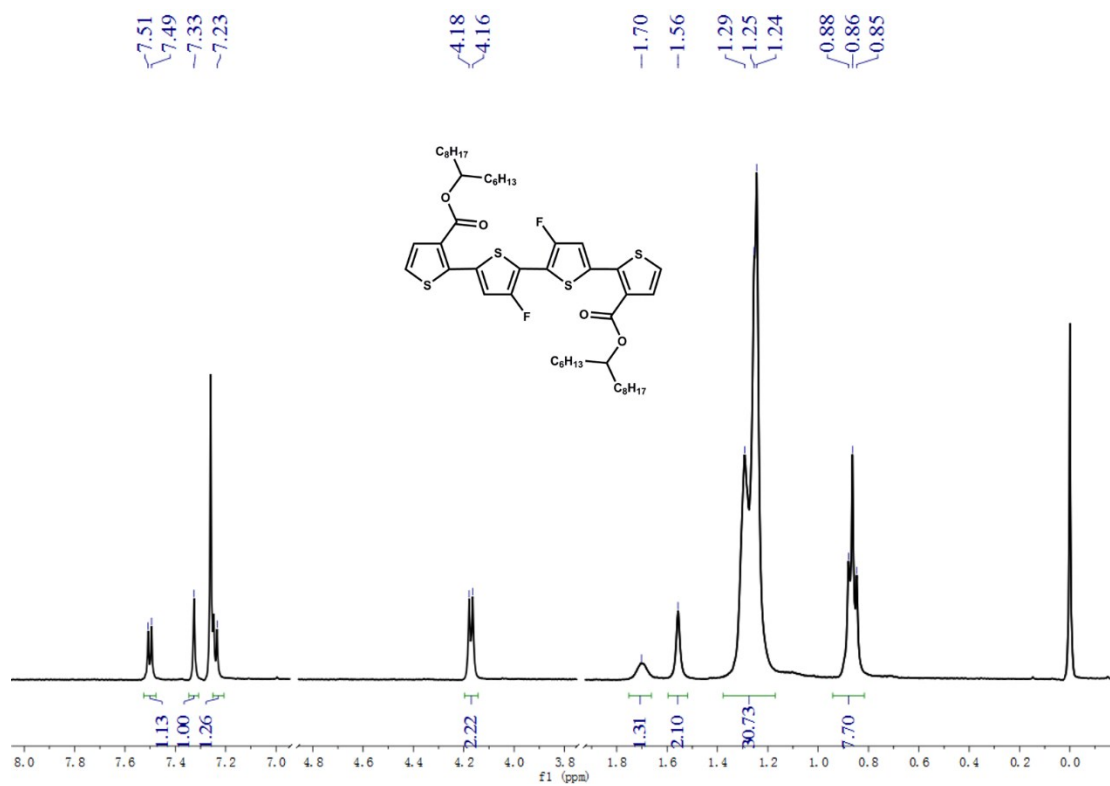


Figure S14. The ¹H NMR of M1.

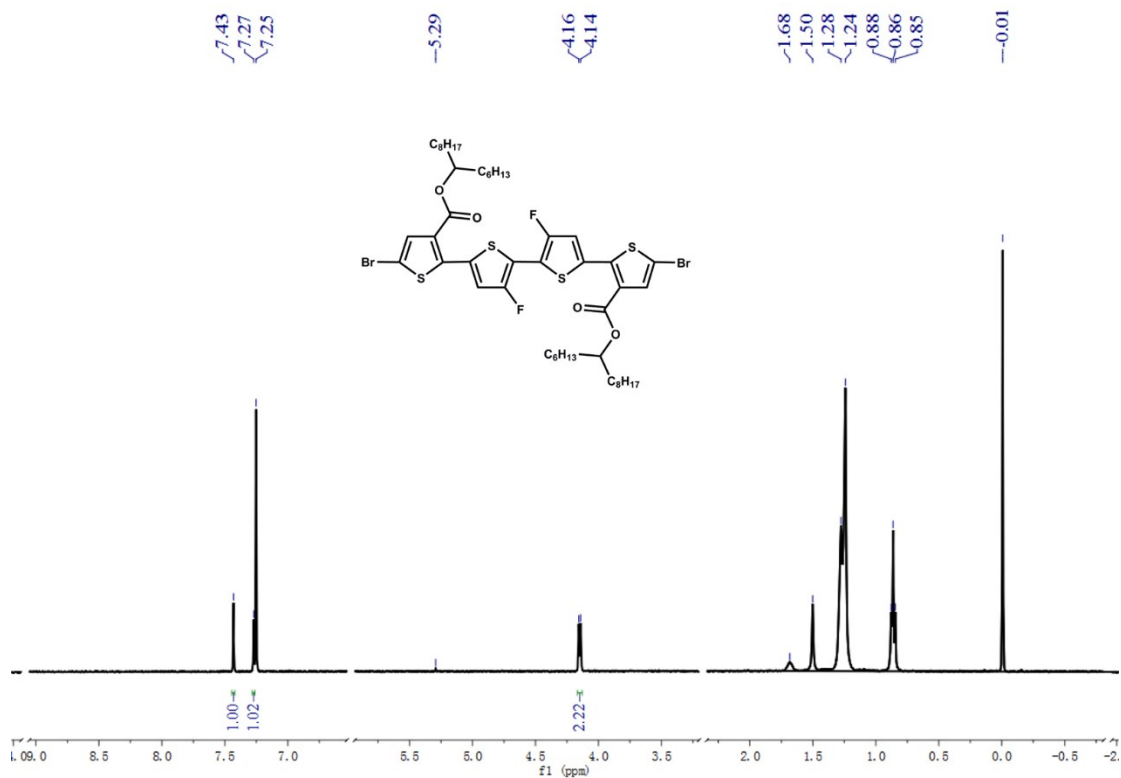


Figure S15. The ¹H NMR of M2.

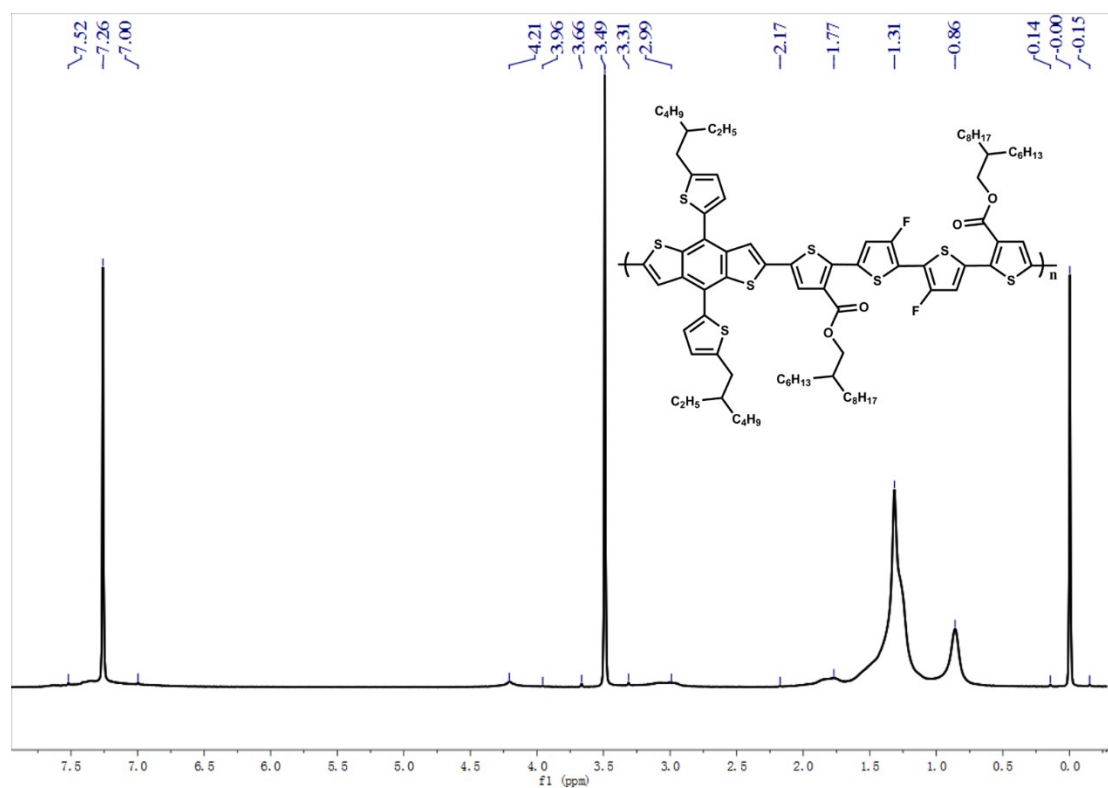


Figure S16. The ¹H NMR of the polymer PBDT-C4T.

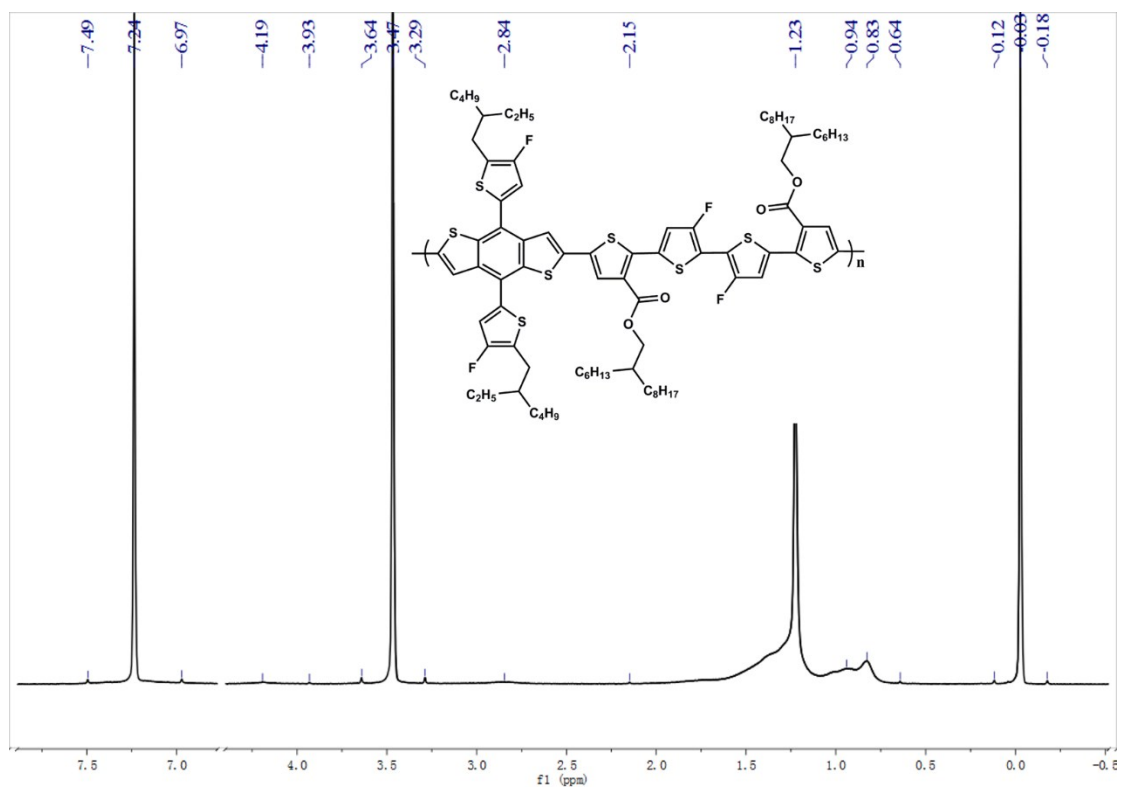


Figure S17. The ^1H NMR of the polymer PBDT-F-C4T.

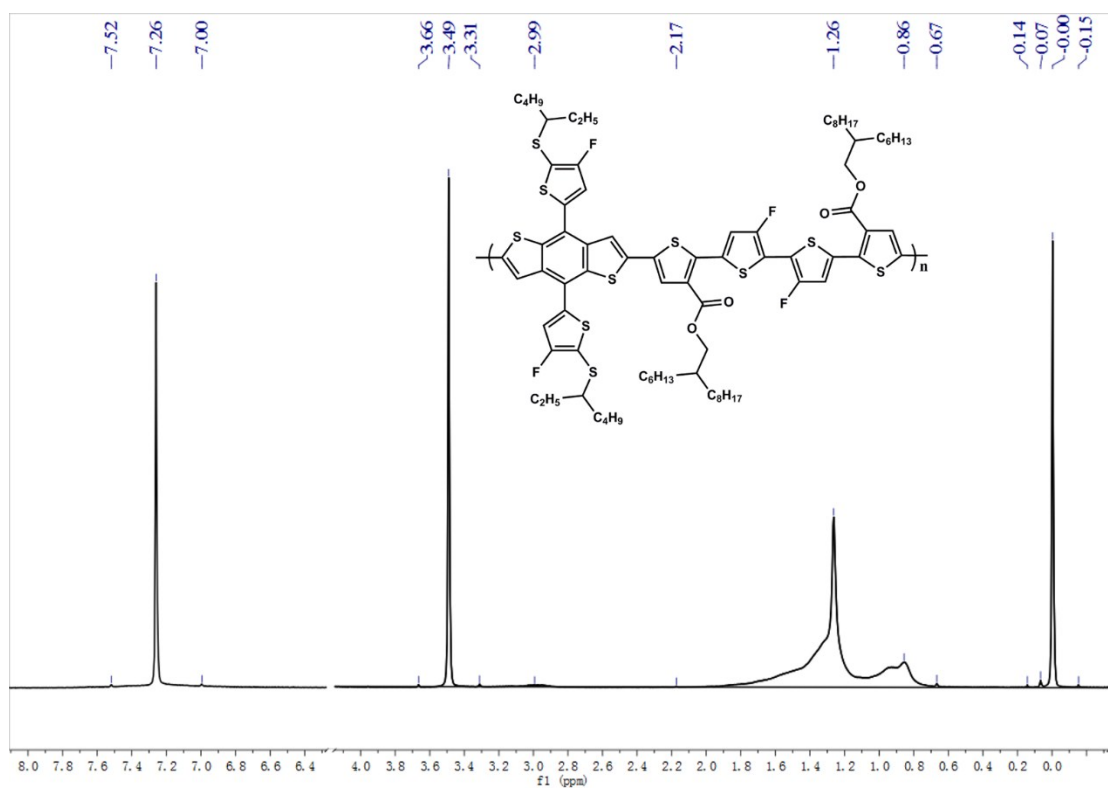


Figure S18. The ^1H NMR of the polymer PBDT-SF-C4T.

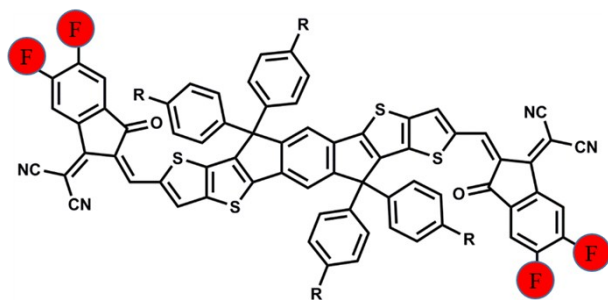


Figure S19. The chemical structure of acceptor IT-4F.

References

1. W. Zhao, S. Zhang, Y. Zhang, S. Li, X. Liu, C. He, Z. Zheng and J. Hou, *Adv. Mater.*, 2018, **30**, 1704837.
2. Z. Liao, Y. Xie, L. Chen, Y. Tan, S. Huang, Y. An, H. S. Ryu, X. Meng, X. Liao, B. Huang, Q. Xie, H. Y. Woo, Y. Sun and Y. Chen, *Adv. Funct. Mater.*, 2019, **29**, 1808828.
3. J. Gao, R. Ming, Q. An, X. Ma, M. Zhang, J. Miao, J. Wang, C. Yang and F. Zhang, *Nano Energy*, 2019, **63**, 103888.
4. Y. Wu, C. An, L. Shi, L. Yang, Y. Qin, N. Liang, C. He, Z. Wang and J. Hou, *Angew. Chem.*, 2018, **130**, 13093-13097.
5. Q. Fan, W. Su, Y. Wang, B. Guo, Y. Jiang, X. Guo, F. Liu, T. P. Russell, M. Zhang and Y. Li, *Sci. China Chem.*, 2018, **61**, 531-537.
6. S. Zhang, Y. Qin, J. Zhu and J. Hou, *Adv. mater.*, 2018, **30**, 1800868.
7. W. Li, L. Ye, S. Li, H. Yao, H. Ade and J. Hou, *Adv. Mater.*, 2018, **30**, 1707170.
8. Y. Cui, H. Yao, L. Hong, T. Zhang, Y. Xu, K. Xian, B. Gao, J. Qin, J. Zhang, Zh. Wei and J. Hou, *Adv. Mater.*, 2019, **31**, 1808356.
9. Q. Fan, Q. Zhu, Z. Xu, W. Su, J. Chen, J. Wu, X. Guo, W. Ma, M. Zhang and Y. Li, *Nano Energy*, 2018, **48**, 413-420.
10. S. Li, L. Ye, W. Zhao, H. Yan, B. Yang, D. Liu, W. Li, H. Ade and J. Hou, *J. Am. Chem. Soc.*, 2018, **140**, 7159-7167.
11. J. Yu, P. Chen, C. W. Koh, H. Wang, K. Yang, X. Zhou, B. Liu, Q. Liao, J. Chen, H. Sun, H. Y. Woo, S. Zhang and X. Guo, *Adv. Sci.*, 2019, **6**, 1801743.
12. H. Yao, Y. Cui, D. Qian, C. S. Ponceca, Jr., A. Honarfar, Y. Xu, J. Xin, Zh. Chen,

- L. Hong, B. Gao, R. Yu, Y. Zu, W. Ma, P. Chabera, T. Pullerits, A. Yartsev, F. Gao and J. Hou, *J. Am. Chem. Soc.*, 2019, **141**, 7743–7750.
13. D. Liu, Y. Zhang, L. Zhan, T.-K. Lau, H. Yin, P. W. K. Fong, S. K. So, S. Zhang, X. Lu, J. Hou, H. Chen, W.-Y. Wong and G. Li, *J. Mater. Chem. A*, 2019, **7**, 14153.
14. W. Zhao, L. Ye, S. Li, X. Liu, S. Zhang, Y. Zhang, M. Ghasemi, C. He H. Ade and J. Hou, *Sci. China Mater.*, 2017, **60**, 697.
15. Z. Zheng, O. M. Awartani, B. Gautam, D. Liu, Y. Qin, W. Li, A. Bataller, K. Gundogdu, H. Ade and J. Hou, *Adv. Mater.*, 2017, **29**, 1604241.
16. J. Wan, X. Xu, G. Zhang, Y. Li, K. Feng and Q. Peng, *Energy Environ. Sci.*, 2017, **10**, 1739-1745.
17. X. Du, B. Liu, L. Li, X. Kong, C. Zheng, H. Lin, Q. Tong, S. Tao and X. Zhang, *J. Mater. Chem., A*, 2018, **6**, 23840-23855.
18. W. Su, G. Li, Q. Fan, Q. Zhu, Xia Guo, J. Chen, J. Wu, W. Ma, M. Zhang and Y. Li, *J. Mater. Chem. A*, 2019, **7**, 2351.
19. X. Xu, T. Yu, Z. Bi, W. Ma, Y. Li and Q. Peng, *Adv. Mater.*, 2018, **30**, 1703973.
20. C. Liao, M. Zhang, X. Xu, F. Liu, Y. Lia and Q. Peng, *J. Mater. Chem. A*, 2019, **7**, 716.
21. Y. Qin, L. Ye, S. Zhang, J. Zhu, B. Yang, H. Ade and J. Hou, *J. Mater. Chem. A*, 2018, **6**, 4324-4330.
22. S. Dong, K. Zhang, B. Xie, J. Xiao, H.-L. Yip, H. Yan, F. Huang and Y. Cao, *Adv. Energy Mater.*, 2019, **9**, 1802832.
23. W. Zhao, S. Zhang, Y. Zhang, S. Li, X. Liu, C. He, Z. Zheng and J. Hou, *Adv. Mater.*, 2018, **30**, 1704837.
24. D. Liu, B. Yang, B. Jang, B. Xu, S. Zhang, C. He, H. Y. Woo and J. Hou, *Energy Environ. Sci.*, 2017, **10**, 546.